Redox Biology 44 (2021) 102020

Contents lists available at ScienceDirect

Redox Biology

journal homepage: www.elsevier.com/locate/redox

Lutein attenuates angiotensin II- induced cardiac remodeling by inhibiting AP-1/IL-11 signaling

Youming Chen [a,1], Lan Wang [b,1], Shixing Huang [c,1], Jiangfeng Ke [d], Qing Wang [e], Zhiwen Zhou [f,**], Wei Chang [g,*]

[a] Department of Cardiology, Shanghai Jiaotong University Affiliated Sixth People's Hospital, Shanghai, China
[b] Department of Radiology, Ruijin Hospital, Shanghai Jiaotong University School of Medicine, Shanghai, China
[c] Department of Cardiovascular Surgery, Ruijin Hospital, Shanghai Jiaotong University School of Medicine, Shanghai, China
[d] Department of Endocrinology and metabolism, Shanghai Jiaotong University Affiliated Sixth People's Hospital, Shanghai, China
[e] Department of Traditional Chinese Medicine, Shanghai Jiaotong University Affiliated Sixth People's Hospital, Shanghai, China
[f] Department of Cardiology, Shanghai Xuhui District Central Hospital & Zhongshan-xuhui Hospital, Shanghai, China
[g] Department of Emergency, Shanghai Xuhui District Central Hospital & Zhongshan-xuhui Hospital, Shanghai, China

ARTICLE INFO

Keywords:
Lutein
Cardiac fibrosis
IL-11
AP-1
Cardiac remodeling

ABSTRACT

Rationale: Oxidative stress plays a critical role in the development of cardiac remodeling and heart failure. Lutein, the predominant nonvitamin A carotenoid, has been shown to have profound effects on oxidative stress. However, the effect of lutein on angiotensin II (Ang II)-induced cardiac remodeling and heart failure remains unknown.

Objective: The aim of this study was to determine whether lutein is involved in cardiac remodeling and to elucidate the underlying molecular mechanisms.

Methods and results: In vitro experiments with isolated neonatal rat cardiomyocytes (NRCMs) and cardiac fibroblasts (CFs) revealed that lutein significantly attenuated Ang II-induced collagen expression in CFs, and cardiomyocyte hypertrophy. The Ang II-induced increases in superoxide generation, inflammation and apoptosis in cultured CFs were strikingly prevented by lutein. In vivo, fibrosis, hypertrophic cardiomyocyte and superoxide generation were analyzed, and lutein was demonstrated to confer resistance to Ang II-induced cardiac remodeling in mice. Mechanistically, RNA sequencing revealed that interleukin-11 (IL-11) expression was significantly upregulated in mouse hearts in response to Ang II infusion and was significantly suppressed in the hearts of lutein-treated mice. Furthermore, IL-11 overexpression blocked the effects of lutein on fibrosis and oxidative stress in CFs and impaired the protective effect of lutein on cardiac remodeling. Notably, we discovered that lutein could reduce Ang II-induced IL-11 expression, at least partly through the regulation of activator protein (AP)-1 expression and activity.

Conclusions: Lutein has potential as a treatment for cardiac remodeling and heart failure via the suppression of IL-11 expression.

1. Introduction

Heart failure is a growing cause of morbidity and mortality worldwide [1]. Hypertensive cardiac remodeling is a common cause of heart failure. Pathological cardiac remodeling is usually characterized by left ventricular hypertrophy and interstitial fibrosis, caused by mechanical stress from neurohumoral stimulation, blood pressure (BP) elevation and growth factors [2,3]. Accumulating evidence has suggested that excessive production of extracellular matrix (ECM) production and fibrosis, which are hallmarks of pathological remodeling, significantly reduce cardiac tissue compliance and lead to contractile dysfunction [4,5]. Therefore, inhibiting hypertensive cardiac remodeling may prevent heart failure progression. However, clinical therapies and interventions that target the ECM and fibrosis remain limited [6].

* Corresponding author.
** Corresponding author.
E-mail addresses: zhouzhiwenufo@sina.com (Z. Zhou), changwei1st@163.com (W. Chang).
[1] Youming Chen, Lan Wang and Shixing Huang contribute equally to this paper.

https://doi.org/10.1016/j.redox.2021.102020
Received 20 April 2021; Received in revised form 17 May 2021; Accepted 20 May 2021
Available online 25 May 2021

The renin-angiotensin-aldosterone system (RAAS) plays a critical role in many cardiovascular diseases. Previous studies have shown that angiotensin II (Ang II) is the main mediator of the RAAS system [7]. Ang II induces a proliferative and migratory phenotype in cardiac fibroblasts (CFs) and leads to the deposition of matrix proteins [8]. In addition, Ang II-induced pathological remodeling is closely associated with impaired autophagy, metabolism, oxidative stress, and apoptosis [9,10]. Blocking the Ang II signaling pathway has been shown to prevent myocardial hypertrophy and fibrosis [11]. Recent studies have showed that Ang II significantly activates the interleukin-11 (IL-11)/extracellular signal-regulated kinase (ERK1/2) signaling pathway [12]. Stuart Cook and colleagues showed that the cytokine IL-11 is crucial in the pathogenesis of cardiac fibrosis [13]. Chronic activation of the IL-11 signaling pathway has been implicated in heart failure, although the exact mechanism is unknown [14,15]. Therefore, negative regulation of these signaling pathways could be clinically beneficial for the treatment of hypertensive heart failure.

Lutein, a natural dihydroxycarotenoid, can be obtained from a wide variety of fruits and vegetables [16]. Dramatically, lutein has been reported to inhibit inflammation in diabetic retinopathy (DR) [17] and coronary artery disease [18] and exert antioxidative effects on cerebrovascular endothelial cells [19] and retinal pigment epithelial (ARPE-19) cells [20]. Moreover, many randomized clinical trials have reported that a lutein-rich diet decreases the incidence of nonalcoholic fatty liver disease [21], age-related macular degeneration (AMD) [22], breast cancer [23] and cognitive dysfunction [24] and reduces the risk of cardiovascular events, including atrial fibrillation [25], atherosclerosis [26] and hypertension [27]. Despite these promising results, the underlying mechanisms remain unclear. Furthermore, the role and mechanisms of lutein in hypertensive cardiac remodeling have not been identified.

In this study, we sought to test the hypothesis that lutein plays a protective role in cardiac remodeling. We challenged mice with Ang II to examine the protective effects of lutein. We discovered that lutein suppressed pathological cardiac remodeling induced by Ang II by inhibiting AP-1/IL-11/ERK signaling.

2. Methods

2.1. Animals and animal models

The studies were approved by the Animal Care and Use Committee of Shanghai Jiao Tong University Affiliated Sixth People's Hospital. All mice were kept in an environment with controlled light cycles, temperature, and humidity. The mice were allowed ad libitum access to food and water. Male mice aged 8–9 weeks (24–26 g) were used for all experiments.

Ang II infusion-induced cardiac remodeling by chronic subcutaneous infusion of Ang II (No. A9525; Sigma-Aldrich) at a dose of 1.4 mg/kg/day dissolved in normal saline using the ALZET Osmotic Pumps (model 2004) for 4 weeks. Control mice were infused with equal volume of normal saline. For Lutein treatment, mice were randomized to be administered with either DMSO or Lutein (Macklin, China) dissolved in 10%DMSO for 28 consecutive days.

2.2. Lentivirus packaging

The coding sequences (CDS) of mouse and rat IL-11 were effused into the backbones of lentivirus overexpressing plasmids pCDH by homologous recombination through the selection of two restriction enzyme cutting sites——the EcoRI and NotI. In order to package lentivirus, the pCDH-mIL-11 and pCDH-rIL-11 plasmids were co-transfected with lentiviral packaging plasmids pCMV-gag/pol and pCMV-VSVG into 293T cell line by lipofectamine 3000, respectively. The suprenatants of transfected 293T cells were collected and the lentivirus precipitate was obtained by ultracentrifugation. After suspension and titer detection, the lentivirus was used in the following in vivo and in vitro experiments.

2.3. Intramyocardial injection of lentivirus (LV)-IL-11

Intramyocardial injection was performed as follows [28]. Male mice aged 8–9 weeks were anaesthetized with 2% isoflurane, and an incision approximately 1 cm long in length was made between the fourth and fifth left ribs to expose the heart. The heart was then squeezed by exerting pressure on the right chest wall. The LV-IL-11 was delivered via five separate intramyocardial injections (5 μl per injection) into the front, side, and back of the left ventricle. The heart was then repositioned in the chest cavity and the chest wall was sutured. Two weeks later, sham and Ang II infusion were performed.

2.4. Isolation and culture of primary cardiomyocytes and CFs, drug treatments, lentivirus construction, transfection and immunofluorescent staining

Primary CFs and NRCMs were isolated from the hearts of 2 to 3-day-old neonatal Sprague-Dawley rats. The heart tissues were cut into about 1 mm^3 and then digested with 0.1% collagenase II (Worthington) and placed at 0.125% Trypsin-EDTA (Gibco, USA) in DMEM at 37 °C for 10 min. The solution of the heart tissue was then transferred to a centrifuge tube containing DMEM plus 10% fetal bovine serum (FBS). A new enzyme solution was added to the tissue, and the procedure repeated 5–7 times. The collected enzyme-solution was filtered through a cellular sifter (200-mesh) and then centrifuged at 1000 rpm for 5 min. Cells were dispersed and plated on 100 mm dishes in 5% CO_2 at 37 °C for 60–90 min to allow non-cardiac myocytes (mainly cardiac fibroblasts) to adhere to the plastic surface. Suspended cardiomyocytes were collected and transferred into 6- or 24-well plates with coated laminin (10 μg/mL). NRCMs were grown in DMEM supplemented with 10% FBS, penicillin (100 U/mL)/streptomycin (100 μg/mL) and 100 μmol/L 5-bromodeoxyuridine (Sigma, #B5002) for 48 h. To induce hypertrophy, NRCMs were cultured in serum-free DMEM for 12 h and treated with Ang II (1 μmol/L; Sigma) for 24 h. Most of the adherent cells were cardiac fibroblasts, which were identified on the basis of vimentin positive expression. Primary cardiac fibroblasts were passaged until cells reached approximately 70%–80% confluence on the plate and were then prepared for further incubation. CFs were grown in DMEM supplemented with 10% FBS, penicillin (100 U/mL)/streptomycin (100 μg/mL) and infected with the lentivirus at a multiplicity of infection (MOI) of 30 in serum-free medium for 6 h. Then, these cells were maintained for 72 h in DMEM. After culture, the cells were serum-deprived for 12 h and then stimulated with Ang II (1 μmol/L) for the indicated times.

Immunofluorescence staining of α-actinin (05–384, Merck Millipore, 1:100 dilution) in NRCMs was performed using established protocols as previously described [29]. The surface areas were measured using a quantitative digital image analysis system (Image-Pro Plus 6.0).

Immunofluorescence staining of alpha-smooth muscle actin (α-SMA) (Abcam, ab7817) in cultured CFs was performed. Briefly, the cells were fixed in 4% paraformaldehyde for 15 min and permeabilized with 0.1% TritonX-100 for 20 min. After being blocked with 5% BSA for 1 h at room temperature, the cells were incubated with primary antibody α-SMA at 4 °C overnight. The cells were rinsed three times with PBS and incubated with secondary antibodies (Beyotime, A0423) for 1 h at room temperature in the dark. The cells were finally rinsed three times and incubated in DAPI (Beyotime, C1005). Images were visualized by using a fluorescence microscope (Nikon, Japan).

2.5. Plasmids construction

The overexpressing plasmids were constructed based on the backbones of pCDNA3.1. The coding sequence(CDS) of rat Jun and Junb were integrated into the plasmid respectively by homologous recombination through the selection of two restriction enzyme cutting sites—the

NheI and EcoRI.

2.6. CCK-8 assay

The viability and proliferation of CFs was examined using a Cell Counting Kit (CCK-8, Beyotime) assay. CFs were seeded in 96-well plates at a density of 5×10^3 cells/well and then treated with different concentrations of the indicated stimuli. Each well was supplemented with 10 μl of CCK-8 reagent, and the cells were further incubated at 37 °C. A microplate reader (BioTek, USA) was used to measure the optical density (OD) values at 450 nm after culture for an additional 2 h.

2.7. Cell migration assay

CFs were plated in serum-free DMEM medium in the top chamber of a 24-well plate ;the lower chambers contained the culture medium with 10% FBS. Twenty-four hours later, all cells on the upper surface of the membrane were washed with PBS. Then, the cells that penetrated the lower chamber were fixed with 4% formalin and staining with 1% crystal violet solution. Quantification was performed by counting the number of migrating cells under a microscope.

2.8. Apoptosis assay

Caspase-3/7 assays were used to measure cell apoptosis. In brief, cells were seeded on glass coverslips in 12-well dishes. Then, apoptosis was analyzed by the caspase-3/7 assay using CellEvent Caspase-3/7 Green Detection Reagent (Roche Diagnostics) according to the manufacturer's instructions. Images were visualized by using a fluorescence microscope (Nikon, Japan).

2.9. Histology and immunohistochemistry

The left ventricular (LV) samples were fixed in 10% formalin, embedded in paraffin and sectioned a thickness of 4-to 5-μm. Hematoxylin and eosin (H&E) was used for histopathological examination and picrosirius red (PSR) staining was used to quantify collagen deposition. The cell area was calculated by measuring 150–200 myocytes in each group. The LV collagen volume fraction was calculated by measuring the percentage of the stained area (red) relative to the total area. For immunohistochemical staining, the heart tissues were incubated with anti-CD68 antibody (Abcam,ab24590,1:250). The expression of CD68 in each sample was calculated as the mean value of three slices in three different sections.

2.10. Echocardiographic measurements

Transthoracic echo-cardiography at the level of the papillary muscles was performed on anaesthetized mice after Ang-II infusion by a Mylab30CV (ESAOTE) ultrasound system equipped with a 15-MHz probe. Parasternal short-axis views were used to record M-mode tracings at the LV midpapillary level to measure LV dimensions. LV ejection fraction (EF%) was calculated as a measure of systolic function as follows: LVEF (%)=(LVEDV-LDESV)/LVEDV × 100. The LV dimensions were obtained from at least three beats and then averaged.

2.11. Measurement of oxidative stress markers and reactive oxygen species (ROS) generation in vivo and in vitro

The intracellular ROS levels in CFs, NRCMs and heart tissues were determined with DHE fluorescent probes. The collected samples were incubated with DHE at 37 °C for 45 min in a light-protected humidified chamber. The fluorescence signals were captured and analyzed under an inverted fluorescence microscope. The activities of superoxide dismutase (SOD, S0101S), glutathione peroxidase (GSH, S0058) and catalase (CAT, S0051) were determined using commercial assay kits according to the manufacturer's instructions (Beyotime, China).

2.12. Terminal dUTP nick end-labeling (TUNEL) staining

Myocardial sections were dewaxed, rehydrated and incubated with recombinant proteinase K for 30 min at room temperature. Then, the sections were blocked with 10% FBS. The heart sections were stained with a TUNEL kit (Roche) according to the manufacturer's protocol. Images were visualized by using a fluorescence microscope (Nikon, Japan).

2.13. RNA sequencing (RNA-seq)

To investigate the molecular mechanism underlying the regulatory effect of lutein on cardiac remodeling, total RNA was extracted from the hearts of Ang II-treated (n = 5) and Ang II + lutein100-treated (n = 5) mice 4 weeks after Ang II infusion. The mRNA library was constructed according to the manufacturer's protocol (VAHTS mRNA-seq V3 Library Prep Kit for Illumina, Vazyme). In brief, 1 μg of total RNA from each sample was used for library construction. After capture and purification, mRNA was fragmented(85 °C, 6 min) into 250-450bp and reverse transcribed. With end repair and adaptor ligation, the library was purified and underwent size selection. A total of 13 PCR cycles were used for the upcoming library amplification. Agencourt AMPure XPTM Beads (Beckman Coulter) were used for purification and sequencing was carried out on a NovaSeqTM(PE150, Illumina).

2.14. Quantitative real-time RT-PCR (RT-qPCR)

RNA was extracted from cultured cells and heart tissues by using TRIzol reagent (TaKaRa, Japan) and reverse transcribed into cDNA using the Transcriptor First Strand cDNA Synthesis Kit (TaKaRa, Japan). RT-qPCR was carried out using SYBR Green (TaKaRa, Japan), and the results were normalized to the gene expression levels of GAPDH.

2.15. Western blot analysis

Proteins were isolated from heart tissue and cultured cells, with RIPA buffer (Beyotime, China). Next, the protein concentration was quantified using a BCA protein assay kit (Beyotime, China). Twenty micrograms of each protein sample was resolved by SDS/PAGE and lectro transferred onto PVDF membranes. The blots were blocked with 5% BSA for 1 h at room temperature and then incubated with primary antibodies, including: collagen I (COL-1), transforming growth factor (TGF)-β_1, atrial natriuretic peptide (ANP), brain natriuretic peptide (BNP), NOX2, NOX4, IL-1β, TNF-α, IL-11 (Abcam), p-c-Jun (#3270), c-Jun (#9165), p-Jun-B (#8053), Jun-B (#3753), ERK1/2 (#4695), p-ERK1/2 (#4370) (Cell Signaling Technology), GAPDH, Histone H3 (Beyotime, China). Antigen-antibody complexes were detected with an ECL protocol using goat anti-rabbit IgG or goat anti-mouse IgG secondary antibodies. All of protein expression levels were normalized to GAPDH. Immunoblots were quantified by densitometry software (Image-Pro Plus).

2.16. Data analysis

All data are presented as the mean ± SEM or the percentage of at least four independent experiments and were analyzed using SPSS 19.0 statistical software or GraphPad Prism 8.0. Student's t-test was used for comparisons between two groups, and one-way ANOVA followed by the Tukey's comparison test was used for comparisons between at least three groups. A P value < 0.05 was considered statistically significant.

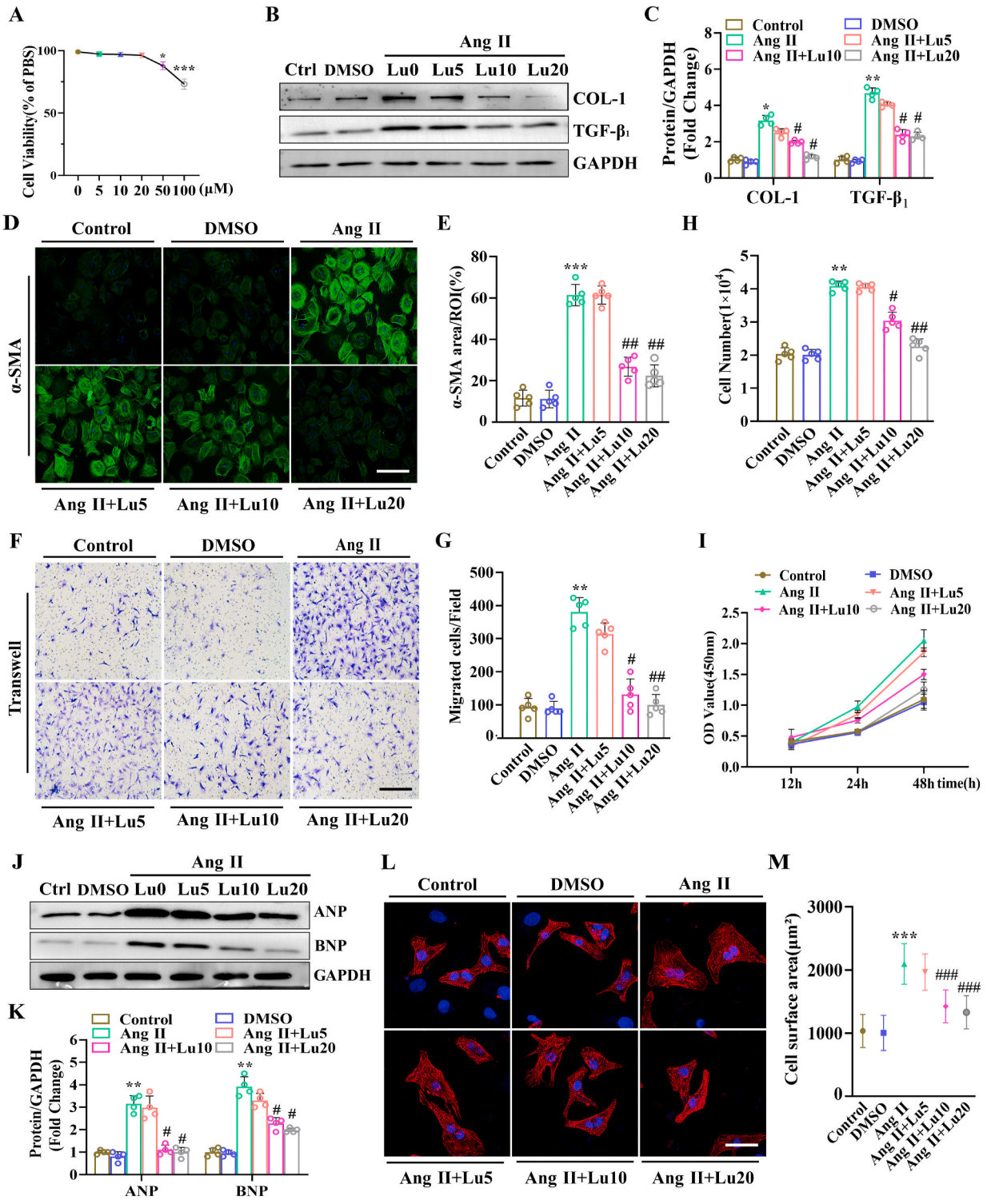

Fig. 1. Lutein prevented Ang II-induced phenotypic transformation in CFs and cardiomyocyte hypertrophy in vitro. (A) CFs were treated with lutein (0, 5, 10, 20, 50 and 100 μM) for 24 h. CCK-8 assays were performed to measure cell viability (n = 4 per experiment). (B, C) CFs were treated with lutein (5, 10 and 20 μM) and Ang II (1 μM) for 24 h. COL-1 and TGF-β_1 expression levels in the heart measured by western blotting, and the expression levels in the different groups were quantified (n = 4 per group). (D, E) Representative immunofluorescence images of α-SMA expression in CFs in response to different treatments (n = 5 in each group, ≥20 fields in each group; green, α-SMA; blue, DAPI; scale bar 50 μm). (F, G) Lutein ameliorated Ang II-induced fibroblast migration, which was quantified visually by an investigator who was blinded to the sample identity (n = 5 in each group). (H, I) Quantification of CF proliferation in response to different treatments by cell counting and CCK-8 assays (n = 5 in each group). (J, K) ANP and BNP expression levels in the heart were measured by Western blotting, and the expression levels in the different groups were quantified (n = 4 per group). (L, M) Representative images of α-actinin (red)- and DAPI (blue)-stained cardiomyocytes in the different groups. (n = 50+ cells per group; red, α-actinin; blue, DAPI; scale bar 20 μm). *P < 0.05, **P < 0.01 and ***P < 0.001 compared to the control group; $^{\#}$P < 0.05, $^{\#\#}$P < 0.01 and $^{\#\#\#}$P < 0.001 compared to the Ang II group. (For interpretation of the references to colour in this figure legend, the reader is referred to the Web version of this article.)

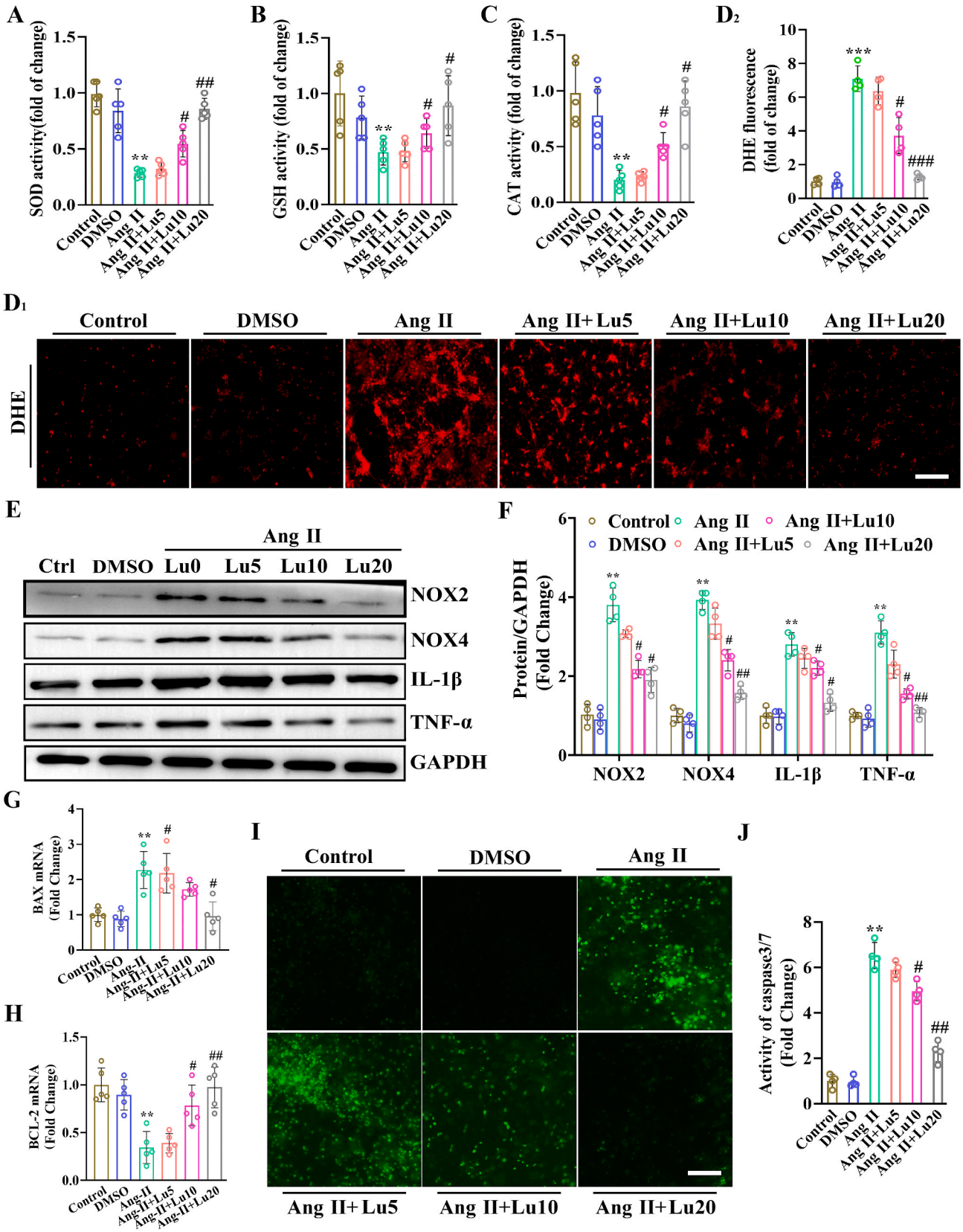

Fig. 2. Lutein suppressed Ang II-induced oxidative stress, inflammation and apoptosis in CFs. (A) SOD activity (n = 5 in each group). (B) GSH activity (n = 5 in each group). (C) CAT activity (n = 5 in each group). (D1) Representative images and (D2) quantitative analysis showing the levels of superoxide anions as measured by DHE staining. (n = 4 in each group). (E, F) Representative blots and quantitative analysis of NOX2, NOX4, IL-1β and TNF-α (n = 4 in each group). (G, H) RT-qPCR analysis of BAX and BCL-2 mRNA levels in primary CFs (n = 5 in each group). (I, J) Analysis of apoptosis in Ang II-induced primary CFs, as indicated by caspase 3 activity, after treatment with lutein for 24 h (Scale bar, 50 μm, n = 5 in each group). *P < 0.05, **P < 0.01 and ***P < 0.001 compared to the control group; $^{\#}$P < 0.05, $^{\#\#}$P < 0.01 and $^{\#\#\#}$P < 0.001 compared to the Ang II group.

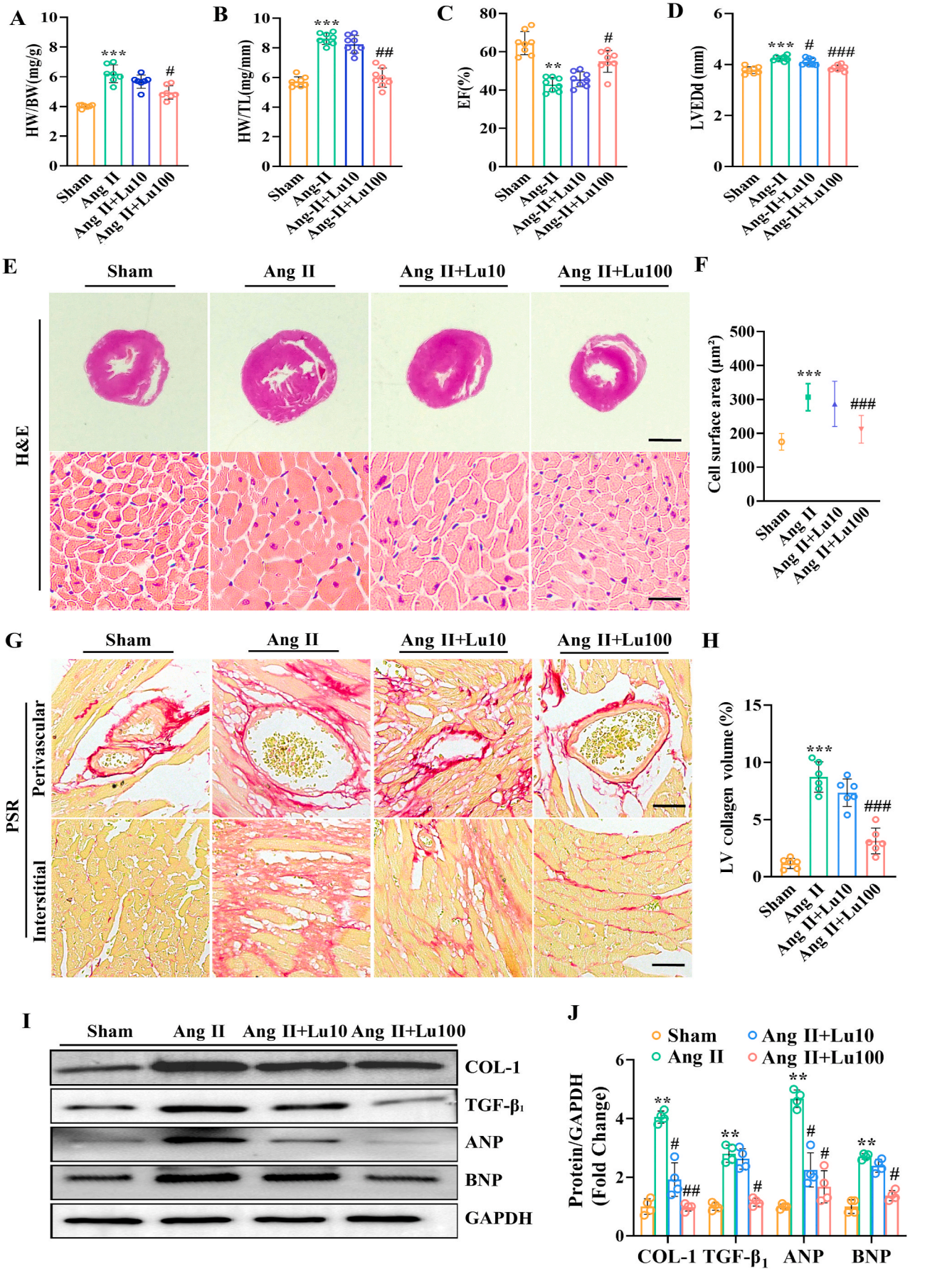

(caption on next page)

Fig. 3. Lutein suppressed Ang II-induced cardiac remodeling in vivo. (A, B) The HW/BW and HW/TL ratios in lutein- and vehicle-treated mice (n = 8 mice per group). (C, D) Echocardiographic assessments of EF% and LVEDd in the indicated groups (n = 8 mice per group). (E) Heart cross-sections were stained with H&E to analyze hypertrophic growth (top row; scale bars, 1 mm) (bottom row; scale bars, 40 mm). (F) Quantification of the average cross-sectional areas of cardiomyocytes in the indicated groups (n ≥ 100 cells per group). (G) Representative images of cardiac fibrosis, as visualized by picrosirius red (PSR) staining of the perivascular area (top; scale bar, 50 μm) and interstitial area (bottom; scale bar, 50 μm). (H) Quantification of the fibrotic area (n = 8 mice per group). (I, J) Western blotting analyses of the protein levels of the fibrotic markers COL-1 and TGF-β_1 and the hypertrophic markers ANP and BNP in the indicated groups (n = 4 mice per group). *P < 0.05, **P < 0.01 and ***P < 0.001 compared to the sham group; $^{\#}$P < 0.05, $^{\#\#}$P < 0.01 and $^{\#\#\#}$P < 0.001 compared to the Ang II group.

3. Results

3.1. Lutein prevented Ang II-induced phenotypic transformation in CFs and cardiomyocyte hypertrophy in vitro

We first examined the effect of lutein on Ang II-induced CF collagen expression and cardiomyocyte hypertrophy in vitro. Cell viability in the presence of lutein was assessed at the 24-h timepoint (Fig. 1A), and we selected lutein concentrations of 5, 10, 20, 50 and 100 μM to assess its effects on CFs. Western blot assays showed that lutein dose-dependently inhibited Ang II-induced COL-1 and TGF-β1 expression in CFs (Fig. 1B–C). Immunofluorescence analysis of α-SMA expression in CFs showed that Ang II-induced CF differentiation (Fig. 1D–E). The effect of lutein on the CF migration was evaluated by performing Transwell assays. Lutein-treated cells exhibited significant reductions in Ang II-induced migration(Fig. 1F–G). Furthermore, treatment with lutein after exposure to Ang II also prevented CF proliferation (Fig. 1H–I). Next, we investigated whether lutein affected cardiomyocyte hypertrophic responses. Cardiomyocyte viability was not affected by 5, 10 and 20 μM lutein (Supplemental Fig. 1A). In NRCMs, Ang II-induced increase in the expression of the hypertrophic markers ANP and BNP was prevented by lutein treatment (Fig. 1J–K). Additionally, we performed α-actinin staining of NRCMs and showed that lutein reduced the increase in cardiomyocyte size (Fig. 1L–M). These results clearly indicated that lutein suppressed Ang II-induced phenotypic transformation in CFs and cardiomyocyte hypertrophy in vitro.

3.2. Lutein inhibited Ang II-induced oxidative stress, inflammation and apoptosis in CFs

Previous studies have shown that cardiac remodeling is closed associated with impairment of oxidative stress, an inflammatory response and apoptosis [30,31]. As shown in Fig. 2A–C, lutein dose-dependently inhibited the downregulation of antioxidant activities, including those of SOD, GSH and CAT, in CFs after Ang II stimulation. We also found that lutein treatment inhibited Ang II-induced ROS generation, as assessed by DHE staining (Fig. 2D). Consistently, NOX2 and NOX4 protein expression was obviously upregulated in Ang II-induced CFs, whereas lutein markedly reversed these changes (Fig. 2E). Furthermore, we explored the effect of lutein on Ang II-induced inflammation in CFs. Western blot analysis showed that Ang II induced obvious upregulation of IL-1β and TNF-α, and these effects were markedly reduced by lutein (Fig. 2E–F). Additionally, RT-qPCR revealed that lutein significantly and dose-dependently inhibited the Ang II-induced increase in BAX expression and increased the expression of the antiapoptotic molecule BCL-2 (Fig. 2G–H). Immunofluorescence analysis of caspase 3 in CFs showed that lutein suppressed Ang II-induced CF apoptosis (Fig. 2I–J). Taken together, these data robustly verified that lutein significantly inhibited Ang II-induced oxidative stress, inflammation and apoptosis in CFs.

3.3. Lutein attenuated Ang II-induced cardiac remodeling in vivo

To determine the effect of lutein on cardiac remodeling and contractile function in vivo, wild-type (WT) mice were randomized and administered either DMSO or lutein (at a dose of 10 or 100 mg/kg daily) and subjected to chronic subcutaneous Ang II infusion for 4 weeks. To test the toxicity and side effects of lutein on the heart, kidney and liver, we used a maximum dose of 100 mg/kg/day in this study. Lutein at a dose of 100 mg/kg/day had almost no toxicity or side effects on the heart, liver or kidney (Supplemental Figs. 2A–F). Compared with that in the Ang II group, the higher dose of lutein (100 mg/kg/day) significantly reversed Ang II-induced cardiac remodeling, which manifested as decreases in the heart weight/body weight (HW/BW) and heart weight/tibia length (HW/TL) ratios (Fig. 3A–B). Furthermore, lutein-treated mice were also protected against Ang II-induced cardiac hypertrophy, as evidenced by an increased EF and decreased left ventricular end-diastolic diameter (LVEDd), compared with those in the Ang II group (Fig. 3C–D). Lutein-treated mice had significantly attenuated cardiomyocyte cross-sectional areas compared with Ang II-induced mice, as shown by histological analysis with H&E staining (Fig. 3E–F). Consistent with these data, lutein-treated mice also exhibited a significant decrease in the average collagen volume compared with that in Ang II-induced mice, as indicated by PSR staining (Fig. 3G–H). Consistently, lutein-treated mice showed marked suppression of Ang II-induced upregulation of COL-1, TGF-β_1, ANP and BNP protein expression (Fig. 3I–J). These results suggested that lutein protected against Ang II-induced pathological cardiac remodeling.

3.4. Lutein rescued Ang II-mediated increases in myocardial oxidative stress, inflammation and apoptosis

We further explored whether lutein could also regulate ROS levels in Ang II-induced cardiac remodeling. The results indicated that Ang II induced an increase in total ROS levels in the hearts of WT mice, whereas this effect was significantly inhibited in lutein-treated mice (Fig. 4A–B). Previous studies have shown that cardiac remodeling is also associated with an inflammatory response [31], and we found that lutein treatment significantly decreased CD68-labeled macrophage infiltration in Ang II-induced mice, as shown by immunohistochemical staining (Fig. 4C–D). Furthermore, we evaluated the effect of lutein on Ang II-induced myocardial apoptosis by TUNEL staining. The results showed that the number of Ang II-induced TUNEL-positive cells was markedly suppressed by lutein (Fig. 4E–F). Consistently, Western blot analysis showed that lutein treatment clearly inhibited the Ang II-induced upregulation of NOX2, NOX4, TNF-α and IL-1β protein expression in mice (Fig. 4G–H). These results suggested that lutein inhibited Ang II-induced myocardial oxidative stress, inflammation and apoptosis in mice, which may be associated with cardioprotective effects.

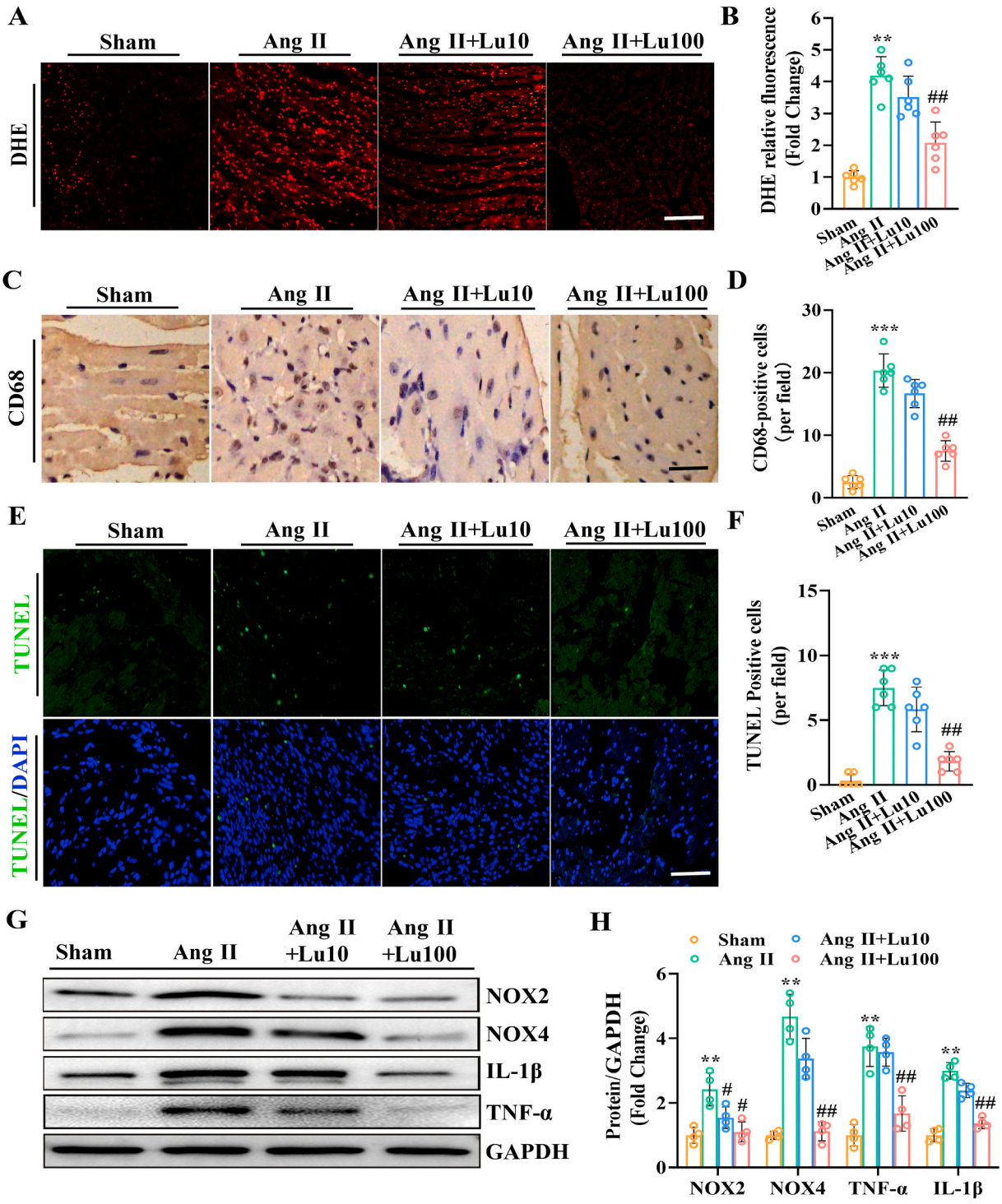

Fig. 4. Lutein inhibited Ang II-induced oxidative stress, inflammation and apoptosis in mice. (A) Representative images and (B) quantitative analysis showing the levels of superoxide anions as measured by DHE staining (n = 5 per group). (C) CD68 expression in mouse hearts in the indicated groups (n = 6 mice per group). (D) Quantification of CD68-positive cells in mouse hearts in the indicated groups. (E) Transferase-mediated deoxyuridine triphosphate-biotin nick end labeling (TUNEL) assay (TUNEL, green; DAPI, blue) (n = 6 per group). (F) Quantification of TUNEL-positive cells in mouse hearts in the indicated groups. (G) Representative blots and (H) quantitative analysis of NOX2, NOX4, IL-1β and TNF-α (n = 4 per group). *P < 0.05, **P < 0.01 and ***P < 0.001 compared to the sham group; $^{\#}$P < 0.05, $^{\#\#}$P < 0.01 and $^{\#\#\#}$P < 0.001 compared to the Ang II group. (For interpretation of the references to colour in this figure legend, the reader is referred to the Web version of this article.)

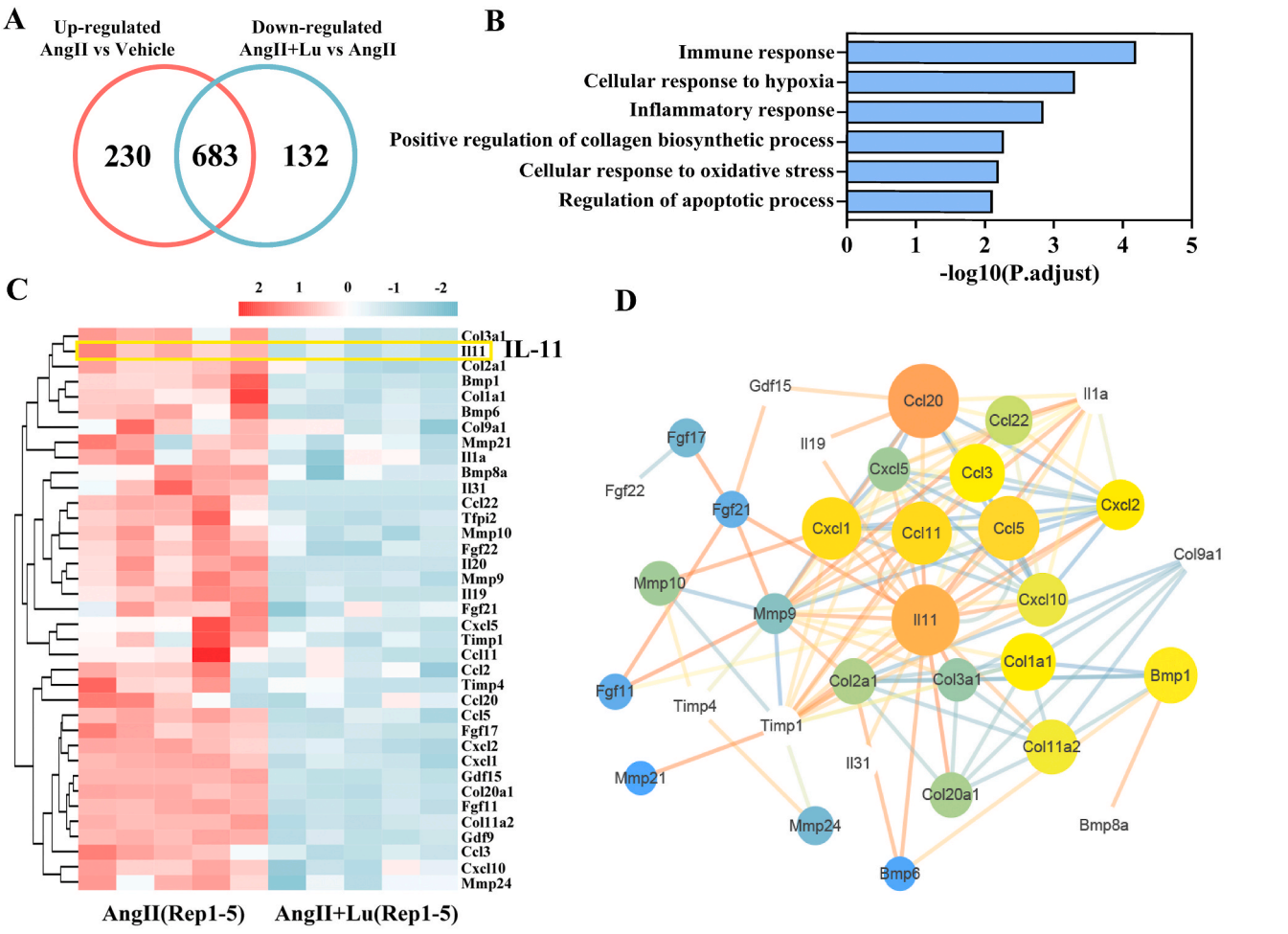

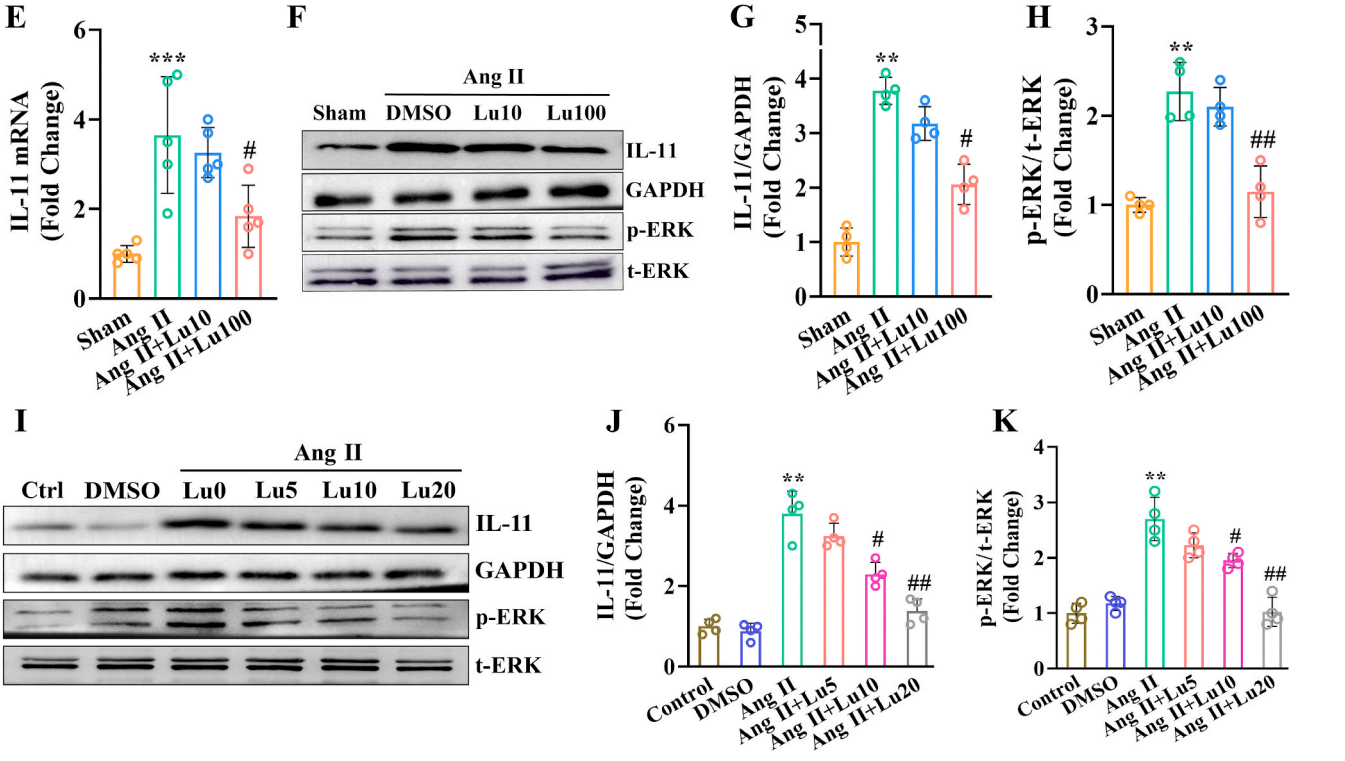

(caption on next page)

Fig. 5. The protective effect of lutein against Ang II-induced cardiac remodeling was associated with the inhibition of IL-11/ERK signaling. (A) An overlap analysis was performed between upregulated genes in the hearts of Ang II-induced mice and downregulated genes in the hearts of lutein-treated mice. (B) Gene ontology (GO) analysis results of 683 genes. (C) Heat map showing the expression patterns of differentially expressed genes that encode secretory proteins. (D) Protein-protein interaction network analysis results of a series of genes encoding secretory proteins. (E) RT-qPCR analysis of the expression of IL-11 in the indicated groups (n = 5 per group). (F) Western blot analysis and (G, H) quantification of the expression of IL-11 and ERK in the indicated groups (n = 4 per group). (I) Western blot analysis and (J, K) quantification of the expression of IL-11 and ERK in the indicated groups (n = 4 per group). In E-H, $^{**}P < 0.01$ and $^{***}P < 0.001$ compared to the sham group; $^{\#}P < 0.05$, $^{\#\#}P < 0.01$ compared to the Ang II group. In I–K, $^{**}P < 0.01$ compared to the control group; $^{\#}P < 0.05$, $^{\#\#}P < 0.01$ compared to the Ang II group.

3.5. Lutein targeted IL-11 to inhibit cardiac remodeling in Ang II-induced mice

To investigate the mechanism underlying the effects of lutein on Ang II-induced cardiac remodeling, we subsequently performed RNA-seq for detailed analysis of the genome-wide gene expression profile in the heart tissues of vehicle-treated mice, Ang II-induced mice and lutein-treated mice. A total of 913 significantly upregulated genes (fold change≥1.5 and corrected P-value≤0.05) were detected in the heart tissues of Ang II-induced mice compared to vehicle-treated mice. Among the 913 upregulated genes, the changes in the expression of 683 genes were significantly reversed in the hearts of lutein-treated mice (Fig. 5A). Among these differentially expressed genes, we performed functional clustering analysis. The results showed that many of the associated biological processes, including the immune response, the cellular response to hypoxia, the inflammatory response, positive regulation of collagen biosynthetic processes, the cellular response to oxidative stress and the regulation of apoptotic processes, were closely associated with cardiac remodeling (Fig. 5B). To further explore the mechanism by which lutein attenuates Ang II-induced cardiac remodeling, we focused on the expression of a series of genes encoding secretory proteins (Fig. 5C). Next, we performed protein-protein interaction network analysis of the genes encoding secretory proteins (Fig. 5D). Based on previous research, we focused on the IL-11 gene. IL-11 is a crucial determinant of cardiovascular fibrosis [12]. Consistent with the RNA-seq results, we verified the altered expression of IL-11 by qPCR and Western blotting in vivo (Fig. 5E–G). Previous studies have shown that IL-11 drives fibrogenic protein expression via noncanonical ERK signaling [12]. Consistently, Western blot analysis showed that lutein treatment decreased p-ERK expression levels compared with those in the Ang II group (Fig. 5F and H). To analyze the potential effects of lutein on IL-11 expression, we performed qPCR analysis of IL-11 in Ang II-induced and lutein-treated cardiomyocytes and CFs. The results showed that lutein suppressed the Ang II-induced IL-11 expression in CFs but not in cardiomyocytes (Figs. S3A–B). Western blot analysis showed that lutein dose-dependently inhibited Ang II-induced ERK expression in CFs (Fig. 5I and K). Taken together, these findings suggested that the protective effect of lutein against Ang II-induced cardiac remodeling was associated with the inhibition of IL-11/ERK signaling.

3.6. Lentivirus-mediated IL-11 overexpression significantly weakened the protective effect of lutein in vitro

To determine the role of IL-11 in lutein-mediated modulation of CFs in vitro, lentivirus-induced IL-11 was used to infect primary CFs (Fig. S4A). IL-11 overexpression prevented the inhibitory effect of lutein on Ang II-induced CF differentiation (Fig. 6A–B), migration (Fig. 6C–D) and proliferation (Fig. 6E–F). RT-qPCR revealed that IL-11 overexpression inhibited lutein-mediated negative regulation of the mRNA levels of COL-1 and TGF-β_1 (Fig. 6G). Furthermore, IL-11 overexpression attenuated the protective effect of lutein on Ang II-induced ROS generation, as shown by DHE staining (Fig. 6H–I). Similar results were also observed for ROS generation, as assessed by measuring the activities of SOD, GSH and CAT (Fig. 6J–L) and RT-qPCR (Fig. 6M). Collectively, these results suggested that IL-11 overexpression significantly weakened the protective effect of lutein in vitro.

3.7. The effects of lutein on Ang II-induced cardiac remodeling were mediated by inhibiting IL-11 expression

To further evaluate the requirement of IL-11 in the protective effect of lutein against cardiac remodeling, IL-11 was overexpressed in cardiac tissue by the injection of a lentivirus harboring the IL-11 gene (LV-IL-11) (Fig. 7A–B). IL-11 overexpression weakened the protective effect of lutein, which manifested as significant increases in the HW/BW ratio (Fig. 7C), HW/TL ratio (Fig. 7D) and LVEDd (Fig. 7E) and a significant decrease in the EF (Fig. 7F) in lutein-treated LV-IL-11 mice compared with lutein-treated LV-GFP mice. Moreover, compared with lutein-treated LV-GFP mice, lutein-treated LV-IL-11 mice exhibited more severe cardiac fibrosis (Fig. 7G–H) and higher ROS levels (Fig. 7I–J). Similar results were also observed for the expression levels of COL-1, TGF-β_1, NOX2 and NOX4 in heart tissues in the different treatment groups (Fig. 7K-L). Taken together, these results suggest that IL-11 overexpression weakened the protective effect of lutein in vivo.

3.8. Lutein suppressed Ang II-induced IL-11 expression by inhibiting AP-1 activity and expression in CFs

Activator protein 1 (AP-1) is a transcription factor complex composed of members of the Fos and Jun families that has been reported to transactivate the IL-11 gene [32–34]. Therefore, we hypothesized that the protective effect of lutein on Ang II-induced cardiac remodeling was associated with AP-1 complex activity. RNA-seq analysis showed that lutein treatment decreased the expression levels of the AP-1 subunits Jun, Junb, Fosl1, Fos and Jund compared with those in the Ang II group (Fig. 8A). RT-qPCR analysis revealed that lu100 inhibited the expression of Jun and Jund but not Fosl1, Fos or Jund compared with Ang II group in mice (Fig. 8B). We further performed a luciferase reporter assay to test whether lutein inhibited AP-1 activity. The luciferase reporter assay showed that lutein dose-dependently inhibited Ang II-induced AP-1 activity (Fig. 8C). By transfecting primary CFs with Jun and Junb overexpression plasmids, we discovered the up-regulated Jun and Junb levels triggered the expressions of IL-11 and p-ERK by western immunoblotting (Fig. 8D–E). We further detected the distribution of p-c-Jun/Jun and p-Jun-B/Jun-B protein in the cytoplasm and nucleus. The results showed that lutein significantly suppressed Ang II-induced the translocation of p-c-Jun and p-Jun-B from the cytoplasm to the nucleus in CFs (Fig. 8F–I). Moreover, Jun and Junb overexpression inhibited the protective effect of lutein against Ang II-induced CF proliferation (Fig. 8J), migration (Fig. 8K) and ROS generation (Fig. 8L–M). Similar results were also observed for the expression levels of COL-1, TGF-β_1, NOX2 and NOX4 in the different treatment groups (Fig. 8N–O). In summary, these results showed that lutein suppressed Ang II-induced IL-11 expression by inhibiting the activity and expression of Jun and Junb.

3.9. The pattern graph of the pathological changes

The pattern graph depicted the working model of lutein-mediated cardioprotection in Ang II-induced cardiac remodeling by inhibiting AP-1/IL-11 signaling (Fig. 9).

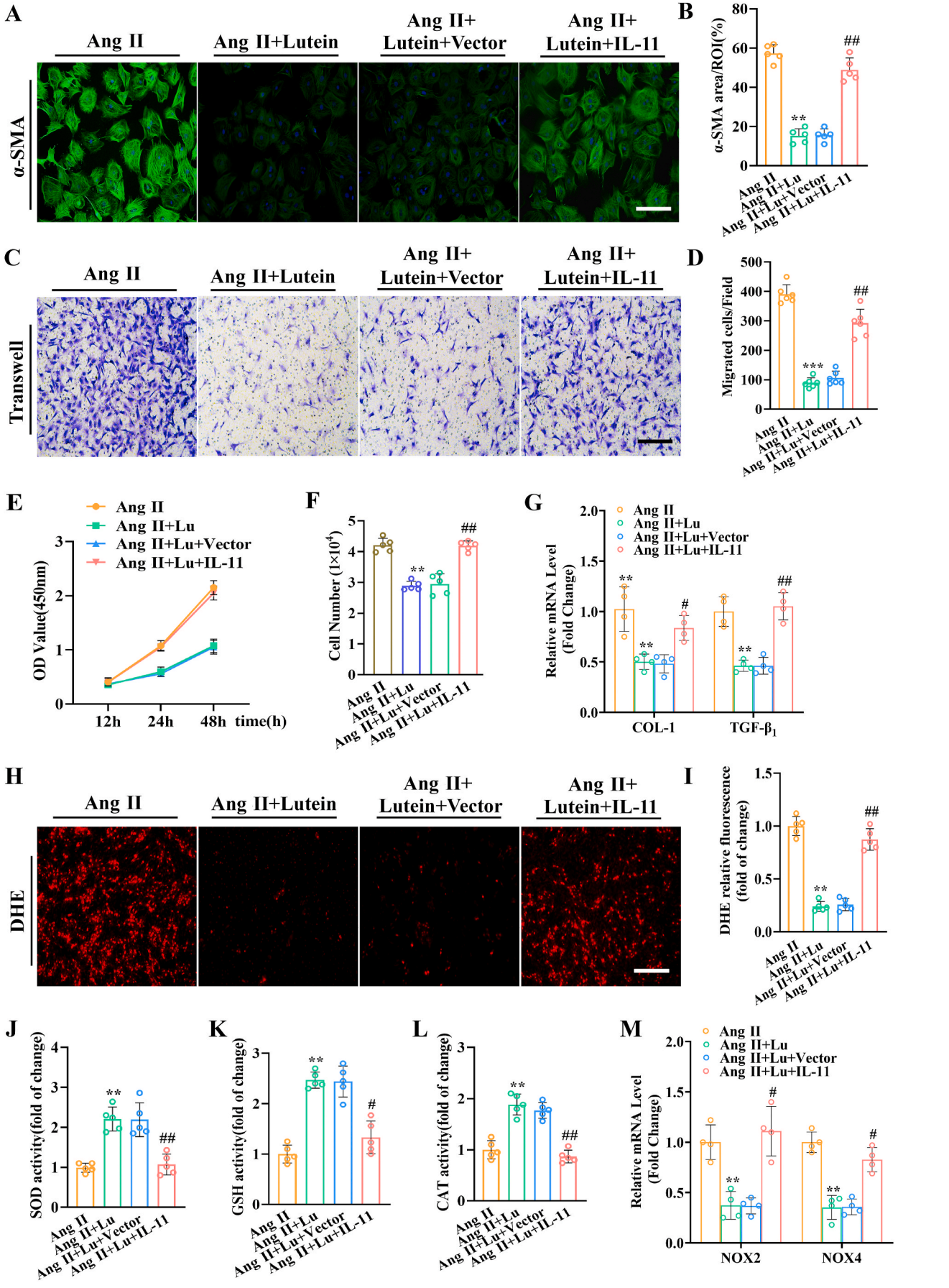

(caption on next page)

Fig. 6. IL-11 overexpression weakened the protective effect of lutein in vitro. (A, B) Representative immunofluorescence images and quantification of α-SMA expression in CFs in response to different treatments (n = 5 in each group, ≥20 fields in each group; green, α-SMA; blue, DAPI; scale bar 50 μm). (C, D) Representative images of the Transwell migration assay and quantification of migrated CFs in the indicated groups (n = 5 in each group). (E, F) Quantification of CF proliferation in response to different treatments as determined by cell counting and CCK-8 assays (n = 5 in each group). (G) The COL-1 and TGF-β_1 mRNA expression levels were measured by RT-qPCR, and the expression levels in the different groups were quantified (n = 4 per group). (H, I) Representative images and quantitative analysis showing the levels of superoxide anions as measured by DHE staining (n = 5 in each group). (J) SOD activity (n = 5 in each group). (K) GSH activity (n = 5 in each group). (L) CAT activity (n = 5 in each group). (M) The NOX2 and NOX4 mRNA expression levels were measured by RT-qPCR, and the expression levels in the different groups were quantified (n = 4 per group). *P < 0.05, **P < 0.01 and ***P < 0.001 compared to the Ang II group; $^{\#}$P < 0.05, $^{\#\#}$P < 0.01 and $^{\#\#\#}$P < 0.001 compared to the Ang II + Lu group. (For interpretation of the references to colour in this figure legend, the reader is referred to the Web version of this article.)

4. Discussion

This study showed that lutein protected against Ang II-mediated deleterious cardiac remodeling by inhibiting the IL-11 protein. In vitro, lutein treatment reduced oxidative stress, proliferation, migration, and phenotypic transformation in cultured neonatal CFs. In vivo, lutein prevented cardiac functional deficits and reduced cardiac fibrosis in Ang II-induced model mice. We further discovered that IL-11 overexpression prevented the protective effects of lutein against Ang II-induced pathological cardiac remodeling. Importantly, lutein suppressed Ang II-induced IL-11 expression by inhibiting the activity and expression of c-Jun/Jun-B.

Pathological cardiac remodeling is usually characterized by alterations in cardiac tissue compliance and the development of end-stage heart failure [35]. Previous studies have shown that the pathological process of cardiac remodeling is associated with reduced contractile function accompanied by a shift in the activation of the neurohumoral system, oxidative stress, endoplasmic reticulum (ER) stress and inflammation [30,31]. Although Ang II receptor blockers, angiotensin converting enzyme inhibitors, diuretics and β-blockers are used to clinically treat pathological cardiac remodeling and heart failure, these drugs are not effective in reversing heart failure [36]. It has been reported that many carotenoids, such as fucoxanthin [37], lycopene [38] and neoxanthin [39], act as antioxidants. Lutein, which is an essential carotenoid, has a protective effect against oxidative stress and inflammation [19,20]. The profound effects of lutein on oxidative stress and inflammation suggest the potential application of lutein in cardiovascular disease. In many clinical trials, low levels of plasma lutein were associated with increased risks of atrial fibrillation [25], atherosclerosis [40] and hypertension [27]. Importantly, lutein supplementation significantly decreased the occurrence and development of many cardiovascular diseases [41,42]. Consistent with these findings, our data demonstrated that lutein prevented and reversed Ang II-induced cardiac dysfunction and remodeling by inhibiting ROS production. In addition, Ang II induced the transdifferentiation of CFs into myofibroblasts, which exhibit high proliferation and migration, resulting in excessive production of ECM and fibrosis, which is a sign of pathological remodeling [35]. Recent studies indicate that carotenoids exhibit therapeutic effects against fibrotic disorders, including chronic kidney disease, pulmonary fibrosis and liver disease [43–45]. In this study, we found that lutein suppressed proliferation, migration and differentiation in vitro and prevented Ang II-induced pathological cardiac fibrosis in vivo. Taken together, these results indicate that lutein protects the heart against Ang II through the attenuation of inflammation, oxidative stress and fibrosis. Previous studies showed that TGF-β_1 is a major driver of pathological cardiac fibrosis and promotes the transition of fibroblasts into activated myofibroblasts [46]. However, there are limitations to targeting TGF-β_1 to reduce cardiac fibrosis due to the pleiotropic roles of TGFβ1 in diverse cell types [47]. Therefore, we need to explore potential drug targets that are downstream of TGF-β_1 with the potential to block fibrosis while avoiding off-target toxicities. Here, an important finding of our study was that lutein inhibited Ang II-induced pathological cardiac remodeling through the suppression of IL-11 expression. Stuart Cook and colleagues showed that the upregulation of cytokine IL-11 was the dominant transcriptional response to Ang II and TGF-β_1 exposure. IL-11 was required for fibroblast activation with all the profibrotic stimuli [13,48]. In mouse models, IL-11 overexpression in heart tissue caused fibrosis whereas genetic deletion of Il11ra1 protected against disease [12,13]. Recently, IL-11 was found to be an important driver of fibrosis in the kidney [15], liver [49] and lung [50]. In the present study, we found that lutein had almost no toxic or side effects on the heart, liver and kidney. We confirmed that lutein suppressed IL-11 expression in the heart in response to Ang II stimulation whereas IL-11 overexpression weakened the protective effects of lutein in vitro and in vivo. Accumulating evidence has suggested that the pathological remodeling response is coordinated with oxidative stress, inflammation, apoptosis and numerous signaling pathways. Jinrui Dong's study showed that IL-11 activity causes hepatocyte death through NOX4-derived ROS, activation of ERK, JNK and caspase-3, impaired mitochondrial function and reduced fatty acid oxidation [51]. Anissa A. Widjaja's study discovered an unexpected proinflammatory role for IL-11 in the liver [49]. In line with the above findings, our current data demonstrated that lutein markedly suppressed Ang II-induced oxidative stress, inflammation and apoptosis in CFs by inhibiting the expression of IL-11. These results revealed inhibiting lutein is a potential therapeutic strategy to treat cardiac fibrosis. Recent observations demonstrated that IL-11, the crucial fibrosis gene acting downstream of TGF-β_1, also activated ERK signaling in heart tissue. Both TGFβ-1 and IL-11 require ERK to induce profibrotic phenotypes [12,50]. In the present study, increased protein levels of TGF-β_1 and IL-1 and ERK phosphorylation were found in the heart in response to Ang II, and these increases were significantly suppressed by lutein supplementation.

AP-1 is a key transcription factor composed of c-Jun, c-Fos and ATF family proteins. Jun proteins (c-Jun, Junb, Jund) homodimerize among themselves or heterodimerize with Fos family proteins (c-Fos, Fosb, Fosl1, Fosl2) to form transcriptionally active AP-1 [52,53]. Previous studies showed that the AP-1 components transactivate the IL-11 promoter by binding to cis elements to increase IL-11 expression [32–34]. Therefore, we speculated that AP-1 was involved in the protective effect of lutein on Ang II-induced cardiac remodeling. Here, an important finding of our study is that lutein protected cardiac fibrosis in response to Ang II through suppression of c-Jun/Jun-B expression and activity. Jun and Fos family proteins played a prominent role in regulating inflammatory reactions [54], oxidative stress [55], and cell survival, proliferation and differentiation [56]. A study by Dan Huang showed that treatment with Ang II promoted the phosphorylation of c-Jun and c-Fos and, enhanced AP-1-driven gene transcription, such as that of COL-1 and COL-3 [57]. A study by Xiaoyang Ho showed that treatment of CFs with Ang II resulted in significant increases in the of c-jun/c-fos heterodimer and the mRNA levels of c-Jun and c-Fos [58]. Ponticos M's study showed that failed degradation of Jun-B contributes to overproduction of type I collagen and development of dermal fibrosis in patients with systemic sclerosis [59]. Our study is the first to show that Ang II-induced cardiac remodeling is associated with increased translocation and expression of p-c-Jun/p-Jun-B to facilitate IL-11 transcription, and this process is suppressed by lutein treatment.

Our study has some limitations, and more research is needed to determine the causative mechanism underlying the protective effects of lutein. First, only two doses were tested in our in vivo study. We need to further study the tissue distribution, concentration and pharmacokinetics of lutein to select the best dose and route of administration. Second, Second, the clinical application needs additional study. More

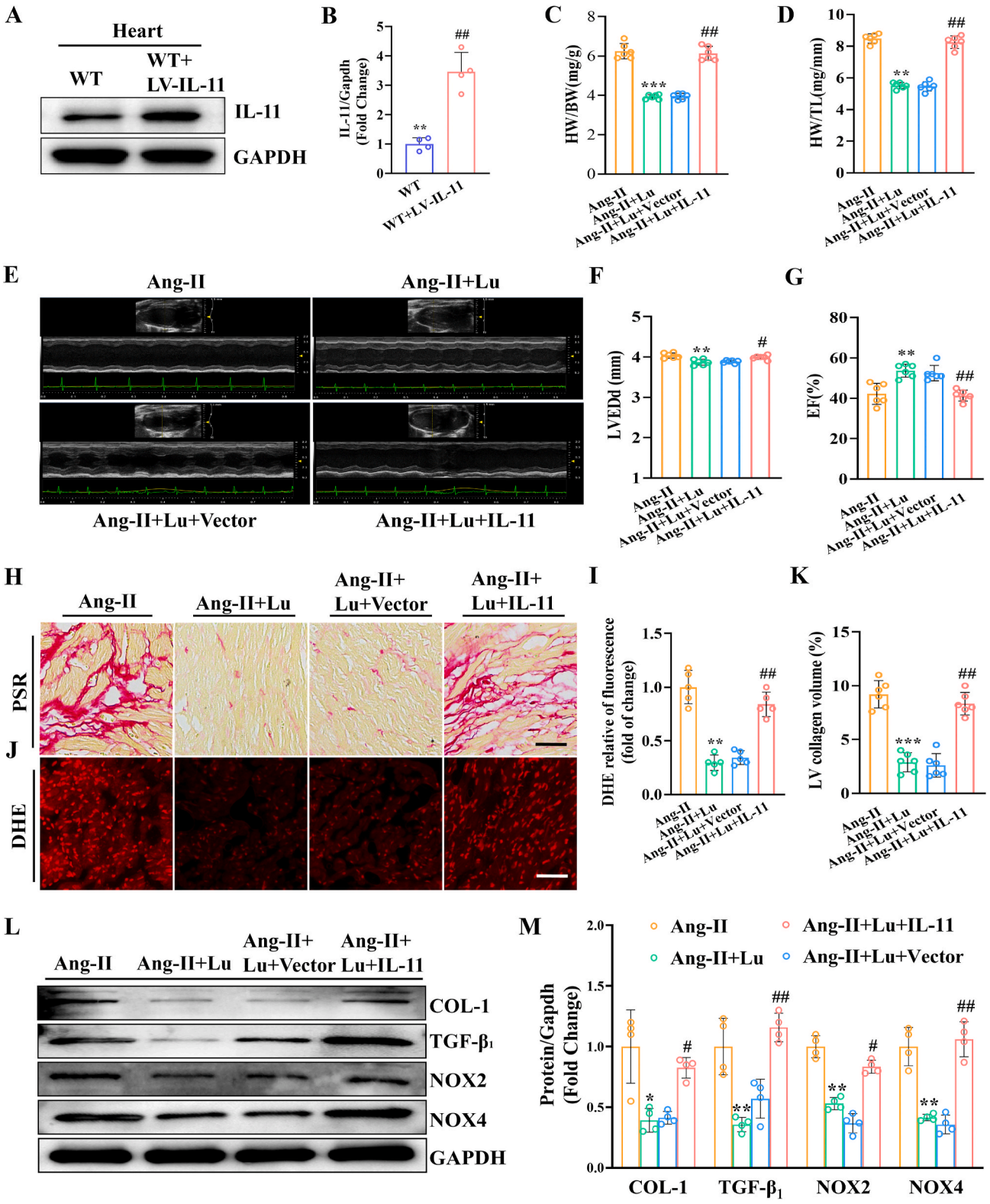

Fig. 7. IL-11 overexpression weakened the protective effect of lutein in vivo. (A) Representative Western blot and (B) quantification of IL-11 levels in the heart tissue of WT mice and LV-IL-11 mice (n = 4 per group). (C, D) The HW/BW and HW/TL ratios in lutein- and vehicle-treated mice (n = 8 per group). (E) Echocardiographic assessments of (F) EF% and (G) LVEDd in the indicated groups (n = 6 per group). (H) Representative images of cardiac fibrosis, as visualized by picrosirius red (PSR) staining of the perivascular area (top; scale bar, 50 μm) (n = 6 per group). (I) Quantification of the fibrotic area (n = 8 per group). (J) Representative images and (K) quantitative analysis showing the levels of superoxide anions as measured by DHE staining (n = 5 per group). (L, M) Western blot analysis of the protein levels of the fibrotic markers COL-1, TGF-β_1, NOX2, and NOX4 in the indicated groups (n = 4 per group). *P < 0.05, **P < 0.01 and ***P < 0.001 compared to the Ang II group; $^{\#}$P < 0.05, $^{\#\#}$P < 0.01 and $^{\#\#\#}$P < 0.001 compared to the Ang II + Lu group.

A

AP-1 family genes

Gene	log_2 fold change	adjusted P-value
Jun	-1.811	3.82E-82
Junb	-1.803	1.02E-75
Fosl1	-1.465	2.38E-44
Fos	-1.273	1.58E-43
Jund	-0.673	4.39E-6

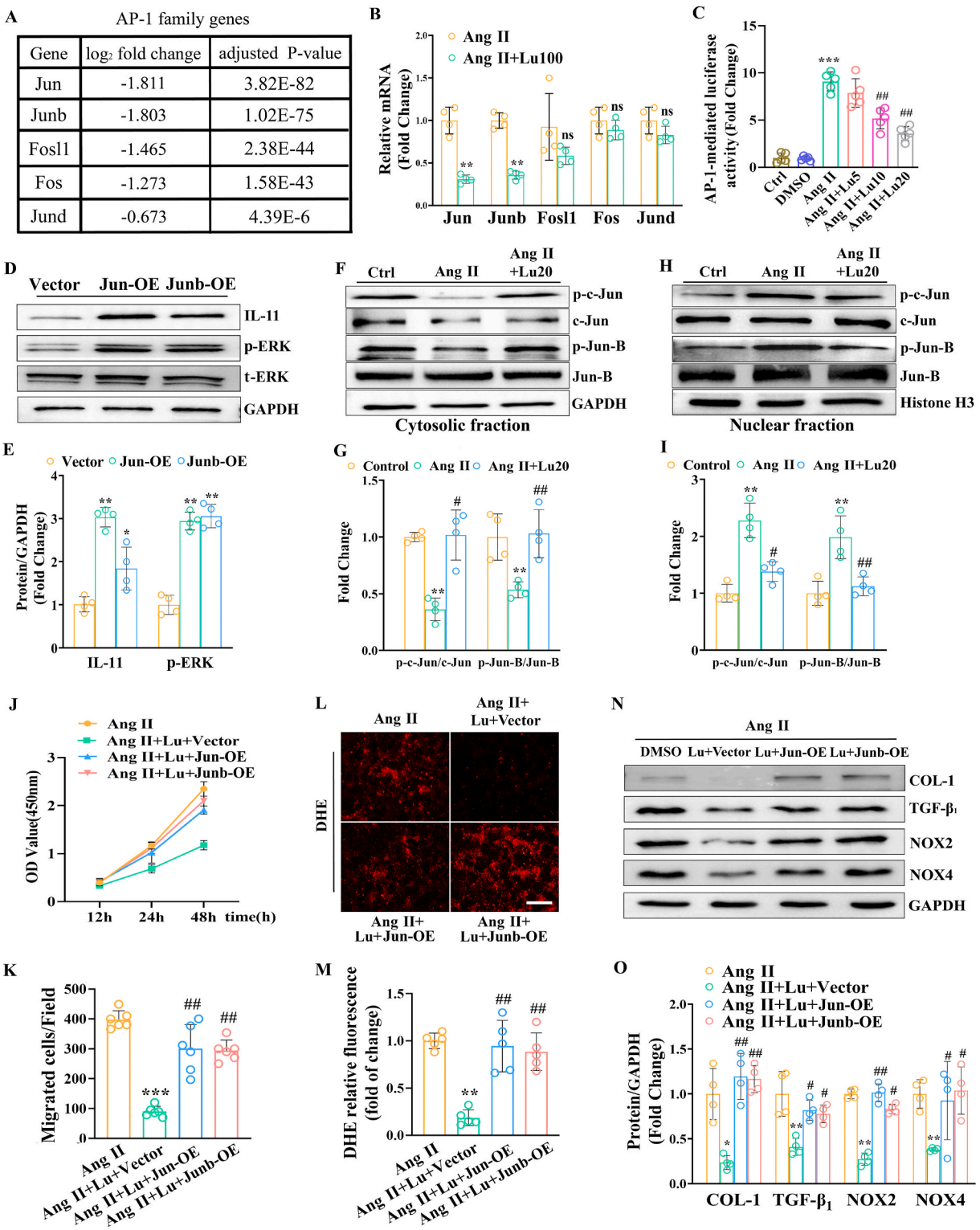

Fig. 8. Lutein suppressed Ang II-induced IL-11 expression by inhibiting the activity and expression of c-Jun/Jun-B in CFs. (A) Changes in the expression of genes belonging to the AP-1 family, as revealed by transcriptomic profiling data. (B) The mRNA expression levels of AP-1 family members, including Fosl1, c-Fos, c-Jun, Junb, and Jund, in CFs in response to different treatments (n = 4 in each group). (C) AP-1-luciferase activity was measured by an AP-1 transcription factor assay kit (n = 5 in each group). (D, E) Representative blots and quantitative analysis of IL-11 and ERK (n = 4 in each group). (F, G) Representative blots and quantitative analysis of p-c-Jun and p-Jun-B (n = 4 in each group). (H, I) Representative blots and quantitative analysis of c-Jun and Jun-B (n = 4 in each group). (J) Quantification of CF proliferation in response to different treatments as determined by CCK-8 assays (n = 5 in each group). (K) Representative images of the Transwell migration assay and quantification of migrated CFs of the indicated groups (n = 5 in each group). (L, M) Representative images and quantitative analysis showing the levels of superoxide anions as measured by DHE staining (n = 5 in each group). (N) Representative blots and (O) quantitative analysis of COL-1, TGF-β_1, NOX2 and NOX4 (n = 4 per group). *P < 0.05, **P < 0.01 and ***P < 0.001 compared to the Ang II group; $^{\#}$P < 0.05, $^{\#\#}$P < 0.01 and $^{\#\#\#}$P < 0.001 compared to the Ang II + Lu + Vector group.

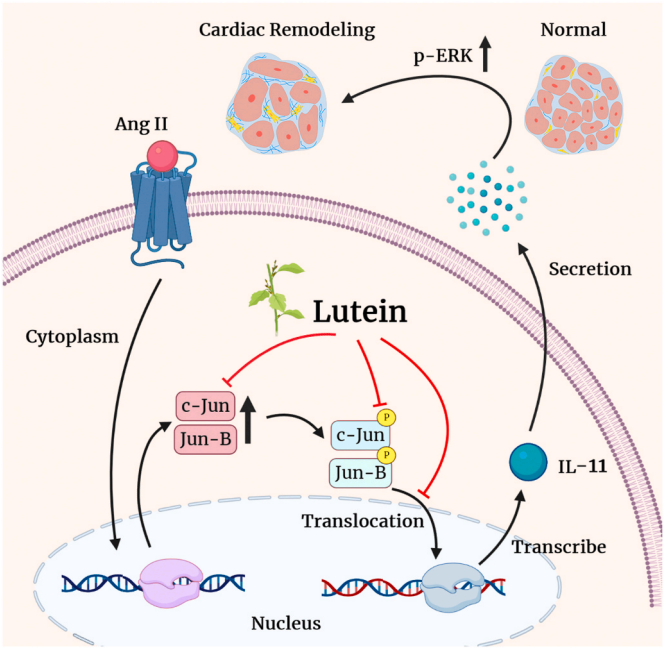

Fig. 9. A working model of lutein-mediated cardioprotection in Ang II-induced cardiac remodeling by inhibiting AP-1/IL-11 signaling.

clinical data are needed to determine the relationship between lutein and hypertension-induced cardiac remodeling. Third, we also found that lutein suppressed Ang II-induced cardiomyocyte hypertrophic responses in vivo and in vitro. However, in vitro experiments revealed that lutein did not affect the expression of IL-11 in cardiomyocytes. It is suggested that the mechanism of lutein in reducing cardiomyocyte hypertrophy may not be through the inhibition of IL-11/ERK signal pathway. Further exploration is needed.

Collectively, our study provides evidence that lutein prevents Ang II-induced cardiac injury via the AP-1/IL-11 pathway. Our study could have implications for the future treatment of cardiac remodeling through the application of lutein.

Declaration of competing interest

The authors declare that they have no conflicts of interest.

Acknowledgements

Youming Chen, Lan Wang and Shixing Huang contribute equally to this paper. This study was supported by Science and Technology Innovation Fundation of Shanghai [No. 20Y11900800], the Key Project of Shanghai Municipal Health Bureau (No.2016ZB0202) and the National Natural Science Foundation of China [No.81570229]. Zhiwen Zhou and Wei Chang conceived and supervised the study.

Appendix A. Supplementary data

Supplementary data to this article can be found online at https://doi.org/10.1016/j.redox.2021.102020.

References

[1] F. Zannad, J.J. McMurray, H. Krum, D.J. van Veldhuisen, K. Swedberg, H. Shi, J. Vincent, S.J. Pocock, B. Pitt, E.-H.S. Group, Eplerenone in patients with systolic heart failure and mild symptoms, N. Engl. J. Med. 364 (2011) 11–21.
[2] V. Rai, P. Sharma, S. Agrawal, D.K. Agrawal, Relevance of mouse models of cardiac fibrosis and hypertrophy in cardiac research, Mol. Cell. Biochem. 424 (2017) 123–145.
[3] M.H. Drazner, The progression of hypertensive heart disease, Circulation 123 (2011) 327.
[4] K. Kis, X. Liu, J.S. Hagood, Myofibroblast differentiation and survival in fibrotic disease, Expet Rev. Mol. Med. 13 (2011) e27.
[5] K.E. Porter, N.A. Turner, CFs: at the heart of myocardial remodeling, Pharmacol. Ther. 123 (2009) 255–278.
[6] N. Hamdani, K.G. Bishu, M. von Frieling-Salewsky, M.M. Redfield, W.A. Linke, Deranged myofilament phosphorylation and function in experimental heart failure with preserved ejection fraction, Cardiovasc. Res. 97 (2013) 464–471.
[7] C.G. Brilla, H. Rupp, R. Funck, B. Maisch, The renin-angiotensin-aldosterone system and myocardial collagen matrix remodelling in congestive heart failure, Eur. Heart J. 16 (Suppl O) (1995 Dec) 107–109.
[8] S. Kim, H. Iwao, Molecular and cellular mechanisms of angiotensin II-mediated cardiovascular and renal diseases, Pharmacol. Rev. 52 (1) (2000 Mar) 11–34.
[9] M. Nakamura, J. Sadoshima, Mechanisms of physiological and pathological cardiac hypertrophy, Nat. Rev. Cardiol. 15 (7) (2018 Jul) 387–407.
[10] S.J. Forrester, G.W. Booz, C.D. Sigmund, T.M. Coffman, T. Kawai, V. Rizzo, R. Scalia, S. Eguchi, Angiotensin II signal transduction: an update on mechanisms of physiology and pathophysiology, Physiol. Rev. 98 (3) (2018 Jul 1) 1627–1738.
[11] C.M. Ferrario, Cardiac remodelling and RAS inhibition, Ther Adv Cardiovasc Dis 10 (3) (2016 Jun) 162–171.
[12] B. Corden, W.W. Lim, W. Song, X. Chen, N.S.J. Ko, L. Su, N.G.Z. Tee, E. Adami, S. Schafer, S.A. Cook, Therapeutic targeting of interleukin-11 signalling reduces pressure overload-induced cardiac fibrosis in mice, J Cardiovasc Transl Res (2020 Jun 26), https://doi.org/10.1007/s12265-020-10054-z. Epub ahead of print. PMID: 32592090.
[13] S. Schafer, S. Viswanathan, A.A. Widjaja, W.W. Lim, A. Moreno-Moral, D. M. DeLaughter, B. Ng, G. Patone, K. Chow, E. Khin, J. Tan, S.P. Chothani, L. Ye, O. J.L. Rackham, N.S.J. Ko, N.E. Sahib, C.J. Pua, N.T.G. Zhen, C. Xie, M. Wang, H. Maatz, S. Lim, K. Saar, S. Blachut, E. Petretto, S. Schmidt, T. Putoczki, N. Guimaräes-Camboa, H. Wakimoto, S. van Heesch, K. Sigmundsson, S.L. Lim, J. L. Soon, V.T.T. Chao, Y.L. Chua, T.E. Tan, S.M. Evans, Y.J. Loh, M.H. Jamal, K. K. Ong, K.C. Chua, B.H. Ong, M.J. Chakaramakkil, J.G. Seidman, C.E. Seidman, N. Hubner, K.Y.K. Sin, S.A. Cook, IL-11 is a crucial determinant of cardiovascular fibrosis, Nature 552 (7683) (2017 Dec 7) 110–115.
[14] J. Ye, Z. Wang, D. Ye, Y. Wang, M. Wang, Q. Ji, Y. Huang, L. Liu, Y. Shi, L. Shi, T. Zeng, Y. Xu, J. Liu, H. Jiang, Y. Lin, J. Wan, Increased interleukin-11 levels are correlated with cardiac events in patients with chronic heart failure, Mediat. Inflamm. (2019 Jan 8) 1575410.
[15] B. Corden, E. Adami, M. Sweeney, S. Schafer, S.A. Cook, IL-11 in cardiac and renal fibrosis: late to the party but a central player, Br. J. Pharmacol. 177 (8) (2020 Apr) 1695–1708.
[16] A. Alves-Rodrigues, A. Shao, The science behind lutein, Toxicol. Lett. 150 (2004) 57–83.
[17] W. Wang, K.C. Tam, T.C. Ng, R.K. Goit, K.L.S. Chan, A.C.Y. Lo, Long-term lutein administration attenuates retinal inflammation and functional deficits in early diabetic retinopathy using the Ins2Akita/+ mice, BMJ Open Diabetes Res Care 8 (1) (2020 Jul), e001519.
[18] R.W.S. Chung, P. Leanderson, A.K. Lundberg, L. Jonasson, Lutein exerts anti-inflammatory effects in patients with coronary artery disease, Atherosclerosis 262 (2017 Jul) 87–93.
[19] T. Liu, W.H. Liu, J.S. Zhao, F.Z. Meng, H. Wang, Lutein protects against β-amyloid peptide-induced oxidative stress in cerebrovascular endothelial cells through modulation of Nrf-2 and NF-κb, Cell Biol. Toxicol. 33 (1) (2017 Feb) 57–67.
[20] A.H. Shivarudrappa, G. Ponesakki, Lutein reverses hyperglycemia-mediated blockage of Nrf2 translocation by modulating the activation of intracellular protein kinases in retinal pigment epithelial (ARPE-19) cells, J Cell Commun Signal 14 (2) (2020 Jun) 207–221.
[21] Y. Lee, S. Hu, Y.K. Park, J.Y. Lee, Health benefits of carotenoids: a role of carotenoids in the prevention of non-alcoholic fatty liver disease, Prev Nutr Food Sci 24 (2) (2019 Jun) 103–113.
[22] Age-Related Eye Disease Study 2 Research Group, Lutein + zeaxanthin and omega-3 fatty acids for age-related macular degeneration: the Age-Related Eye Disease Study 2 (AREDS2) randomized clinical trial, J. Am. Med. Assoc. 309 (19) (2013 May 15) 2005–2015.
[23] A.H. Eliassen, S.J. Hendrickson, L.A. Brinton, J.E. Buring, H. Campos, Q. Dai, J. F. Dorgan, A.A. Franke, Y.T. Gao, M.T. Goodman, G. Hallmans, K.J. Helzlsouer, J. Hoffman-Bolton, K. Hultén, H.D. Sesso, A.L. Sowell, R.M. Tamimi, P. Toniolo, L. R. Wilkens, A. Winkvist, A. Zeleniuch-Jacquotte, W. Zheng, S.E. Hankinson, Circulating carotenoids and risk of breast cancer: pooled analysis of eight prospective studies, J. Natl. Cancer Inst. 104 (24) (2012 Dec 19) 1905.
[24] M.C. Morris, Y. Wang, L.L. Barnes, D.A. Bennett, B. Dawson-Hughes, S.L. Booth, Nutrients and bioactives in green leafy vegetables and cognitive decline: prospective study, Neurology 90 (3) (2018 Jan 16) e214–e222.
[25] J. Karppi, S. Kurl, T.H. Mäkikallio, K. Ronkainen, J.A. Laukkanen, Eur. J. Epidemiol. 28 (1) (2013 Jan) 45–53.
[26] A. Alves-Rodrigues, B. Thomas, The role of lutein in the prevention of atherosclerosis, J. Am. Coll. Cardiol. 40 (4) (2002 Aug 21) 835, author reply 835-6.
[27] Z. Li, J. Chen, D. Zhang, Association between dietary carotenoid intakes and hypertension in adults: National Health and Nutrition Examination Survey 2007-2014, J. Hypertens. 37 (12) (2019 Dec) 2371–2379.
[28] B. Zhang, P. Zhang, Y. Tan, P. Feng, Z. Zhang, H. Liang, W. Duan, Z. Jin, X. Wang, J. Liu, E. Gao, S. Yu, D. Yi, Y. Sun, W. Yi, C1q-TNF-related protein-3 attenuates pressure overload-induced cardiac hypertrophy by suppressing the p38/CREB pathway and p38-induced ER stress, Cell Death Dis. 10 (7) (2019 Jul 8) 520.

[29] K.Q. Deng, J. Li, Z.G. She, J. Gong, W.L. Cheng, F.H. Gong, X.Y. Zhu, Y. Zhang, Z. Wang, H. Li, Restoration of circulating MFGE8 (milk fat globule-EGF factor 8) attenuates cardiac hypertrophy through inhibition of Akt pathway, Hypertension 70 (4) (2017 Oct) 770–779.
[30] L. Bacmeister, M. Schwarzl, S. Warnke, B. Stoffers, S. Blankenberg, D. Westermann, D. Lindner, Inflammation and fibrosis in murine models of heart failure, Basic Res. Cardiol. 114 (3) (2019 Mar 18) 19.
[31] Z.Z. Zhang, W. Wang, H.Y. Jin, X. Chen, Y.W. Cheng, Y.L. Xu, B. Song, J. M. Penninger, G.Y. Oudit, J.C. Zhong, Apelin is a negative regulator of angiotensin II-mediated adverse myocardial remodeling and dysfunction, Hypertension 70 (6) (2017 Dec) 1165–1175, https://doi.org/10.1161/HYPERTENSIONAHA.117.10156. Epub 2017 Oct 3. PMID: 28974565.
[32] W. Tang, L. Yang, Y.C. Yang, S.X. Leng, J.A. Elias, Transforming growth factor-beta stimulates interleukin-11 transcription via complex activating protein-1-dependent pathways, J. Biol. Chem. 273 (10) (1998 Mar 6) 5506–5513.
[33] A. Rauch, S. Seitz, U. Baschant, A.F. Schilling, A. Illing, B. Stride, M. Kirilov, V. Mandic, A. Takacz, R. Schmidt-Ullrich, S. Ostermay, T. Schinke, R. Spanbroek, M.M. Zaiss, P.E. Angel, U.H. Lerner, J.P. David, H.M. Reichardt, M. Amling, G. Schütz, J.P. Tuckermann, Glucocorticoids suppress bone formation by attenuating osteoblast differentiation via the monomeric glucocorticoid receptor, Cell Metabol. 11 (6) (2010 Jun 9) 517–531.
[34] X. Zhang, H. Wu, J.R. Dobson, G. Browne, D. Hong, J. Akech, L.R. Languino, G. S. Stein, J.B. Lian, Expression of the IL-11 gene in metastatic cells is supported by Runx2-Smad and Runx2-cJun complexes induced by TGF-β_1, J. Cell. Biochem. 116 (9) (2015 Sep) 2098–2108.
[35] N.G. Frangogiannis, The extracellular matrix in ischemic and nonischemic heart failure, Circ. Res. 125 (1) (2019 Jun 21) 117–146.
[36] G. Cohuet, H. Struijker-Boudier, Mechanisms of target organ damage caused by hypertension: therapeutic potential, Pharmacol. Ther. 111 (1) (2006 Jul) 81–98.
[37] Y.F. Chiang, H.Y. Chen, Y.J. Chang, Y.H. Shih, T.M. Shieh, K.L. Wang, S.M. Hsia, Protective effects of fucoxanthin on high glucose- and 4-hydroxynonenal (4-HNE)-induced injury in human retinal pigment epithelial cells, Antioxidants (Basel) 9 (12) (2020 Nov 25) 1176.
[38] J. Cheng, B. Miller, E. Balbuena, A. Eroglu, Lycopene protects against smoking-induced lung cancer by inducing base excision repair, Antioxidants (Basel) 9 (7) (2020 Jul 21) 643.
[39] L. Dall'Osto, S. Cazzaniga, H. North, A. Marion-Poll, R. Bassi, The Arabidopsis aba4-1 mutant reveals a specific function for neoxanthin in protection against photooxidative stress, Plant Cell 19 (3) (2007 Mar) 1048–1064.
[40] Z. Zou, X. Xu, Y. Huang, X. Xiao, L. Ma, T. Sun, P. Dong, X. Wang, X. Lin, High serum level of lutein may be protective against early atherosclerosis: the Beijing atherosclerosis study, Atherosclerosis 219 (2) (2011 Dec) 789–793.
[41] F. Hajizadeh-Sharafabad, Z. Ghoreishi, V. Maleki, A. Tarighat-Esfanjani, Mechanistic insights into the effect of lutein on atherosclerosis, vascular dysfunction, and related risk factors: a systematic review of in vivo, ex vivo and in vitro studies, Pharmacol. Res. 149 (2019 Nov) 104477.
[42] M.X. Wang, J.H. Jiao, Z.Y. Li, R.R. Liu, Q. Shi, L. Ma, Lutein supplementation reduces plasma lipid peroxidation and C-reactive protein in healthy nonsmokers, Atherosclerosis 227 (2) (2013 Apr) 380–385.
[43] X. Xie, Q. Chen, J. Tao, Astaxanthin promotes Nrf2/ARE signaling to inhibit HG-induced renal fibrosis in GMCs, Mar. Drugs 16 (4) (2018 Apr 5) 117.
[44] H. Chen, J. Wang, R. Li, C. Lv, P. Xu, Y. Wang, X. Song, J. Zhang, Astaxanthin attenuates pulmonary fibrosis through lncITPF and mitochondria-mediated signal pathways, J. Cell Mol. Med. 24 (17) (2020 Sep) 10245–10250.
[45] Y. Ni, F. Zhuge, M. Nagashimada, N. Nagata, L. Xu, S. Yamamoto, N. Fuke, Y. Ushida, H. Suganuma, S. Kaneko, T. Ota, Lycopene prevents the progression of lipotoxicity-induced nonalcoholic steatohepatitis by decreasing oxidative stress in mice, Free Radic. Biol. Med. 152 (2020 May 20) 571–582.
[46] A. Leask, Potential therapeutic targets for cardiac fibrosis: TGFbeta, angiotensin, endothelin, CCN2, and PDGF, partners in fibroblast activation, Circ. Res. 106 (11) (2010 Jun 11) 1675–1680.
[47] R.J. Akhurst, A. Hata, Targeting the TGF-β_1 signalling pathway in disease, Nat. Rev. Drug Discov. 11 (10) (2012 Oct) 790–811.
[48] I. Fernández-Ruiz, Cardioprotection: IL-11 is a potential therapeutic target in cardiovascular fibrosis, Nat. Rev. Cardiol. 15 (1) (2018 Jan) 1.
[49] A.A. Widjaja, B.K. Singh, E. Adami, S. Viswanathan, J. Dong, G.A. D'Agostino, B. Ng, W.W. Lim, J. Tan, B.S. Paleja, M. Tripathi, S.Y. Lim, S.G. Shekeran, S. P. Chothani, A. Rabes, M. Sombetzki, E. Bruinstroop, L.P. Min, R.A. Sinha, S. Albani, P.M. Yen, S. Schafer, S.A. Cook, Inhibiting interleukin 11 signaling reduces hepatocyte death and liver fibrosis, inflammation, and steatosis in mouse models of nonalcoholic steatohepatitis, Gastroenterology 157 (3) (2019 Sep) 777–792, e14.
[50] B. Ng, J. Dong, G. D'Agostino, S. Viswanathan, A.A. Widjaja, W.W. Lim, N.S.J. Ko, J. Tan, S.P. Chothani, B. Huang, C. Xie, C.J. Pua, A.M. Chacko, N. Guimarães-Camboa, S.M. Evans, A.J. Byrne, T.M. Maher, J. Liang, D. Jiang, P.W. Noble, S. Schafer, S.A. Cook, Interleukin-11 is a therapeutic target in idiopathic pulmonary fibrosis, Sci. Transl. Med. 11 (511) (2019 Sep 25), eaaw1237.
[51] J. Dong, S. Viswanathan, E. Adami, B.K. Singh, S.P. Chothani, B. Ng, W.W. Lim, J. Zhou, M. Tripathi, N.S.J. Ko, S.G. Shekeran, J. Tan, S.Y. Lim, M. Wang, P.M. Lio, P.M. Yen, S. Schafer, S.A. Cook, A.A. Widjaja, Hepatocyte-specific IL11 cis-signaling drives lipotoxicity and underlies the transition from NAFLD to NASH, Nat. Commun. 12 (1) (2021 Jan 4) 66.
[52] C. Abate, T. Curran, Encounters with fos and jun on the road to AP-1, Semin. Canc. Biol. 1 (1) (1990 Feb) 19–26.
[53] S. Sanyal, D.J. Sandstrom, C.A. Hoeffer, M. Ramaswami, AP-1 functions upstream of CREB to control synaptic plasticity in Drosophila, Nature 416 (6883) (2002 Apr 25) 870–874.
[54] E.F. Wagner, Bone development and inflammatory disease is regulated by AP-1 (Fos/Jun), Ann. Rheum. Dis. 69 (Suppl 1) (2010 Jan) i86–88.
[55] W.M. Toone, B.A. Morgan, N. Jones, Redox control of AP-1-like factors in yeast and beyond, Oncogene 20 (19) (2001 Apr 30) 2336–2346.
[56] D. Tewari, S.F. Nabavi, S.M. Nabavi, A. Sureda, A.A. Farooqi, A.G. Atanasov, R. A. Vacca, G. Sethi, A. Bishayee, Targeting activator protein 1 signaling pathway by bioactive natural agents: possible therapeutic strategy for cancer prevention and intervention, Pharmacol. Res. 128 (2018 Feb) 366–375.
[57] D. Huang, Y. Wang, C. Yang, Y. Liao, K. Huang, Angiotensin II promotes poly(ADP-ribosyl)ation of c-Jun/c-Fos in CFs, J. Mol. Cell. Cardiol. 46 (1) (2009 Jan) 25–32.
[58] X. Hou, Y. Zhang, Y.H. Shen, T. Liu, S. Song, L. Cui, P. Bu, PPAR-γ activation by rosiglitazone suppresses angiotensin II-mediated proliferation and phenotypictransition in CFs via inhibition of activation of activator protein 1, Eur. J. Pharmacol. 715 (1–3) (2013 Sep 5) 196–203.
[59] M. Ponticos, I. Papaioannou, S. Xu, A.M. Holmes, K. Khan, C.P. Denton, G. Bou-Gharios, D.J. Abraham, Failed degradation of JunB contributes to overproduction of type I collagen and development of dermal fibrosis in patients with systemic sclerosis, Arthritis Rheum. 67 (1) (2015 Jan) 243–253.